Supplement of Atmos. Chem. Phys., 25, 16983–17007, 2025 https://doi.org/10.5194/acp-25-16983-2025-supplement © Author(s) 2025. CC BY 4.0 License.





## Supplement of

Unexpectedly persistent  $PM_{2.5}$  pollution in the Pearl River Delta, South China, in the 2015–2017 cold seasons: the dominant role of meteorological changes during the El Niño-to-La Niña transition over emission reduction

Kun Qu et al.

Correspondence to: Xuesong Wang (xswang@pku.edu.cn) and Yuanhang Zhang (yhzhang@pku.edu.cn)

The copyright of individual parts of the supplement might differ from the article licence.

## S1. Evaluation of the model's performance in meteorological simulations

As listed in Table S3, the mean bias (MB) for air temperature and absolute humidity indicates that these variables in East China were only slightly underestimated by 0.1–0.3 K and 0–0.7 g/kg, respectively. The high index of agreement (IOA; > 0.96 in this study) further suggests the model's good capacity in reproducing the spatiotemporal variations of these variables during the cold seasons. For wind speed, the MB, root mean square error (RMSE) and IOA all fall within the recommended ranges, which is indicative of a satisfying model performance. However, the gross errors (GE) for wind direction over the six months nearly all exceed the recommended benchmark of 30°. Similar findings have been reported in other simulation studies (e.g., Borge et al., 2008; Wang et al., 2010; Zhang et al., 2012; Hu et al., 2016), where GE values below 30° for wind direction simulations are rarely achieved. In this study, the GE values are comparable or better than those reported in previous studies, suggesting that the performance in simulating wind direction is also acceptable.

In summary, the WRF model demonstrates strong performance in meteorological simulations based on the statistical metrics in Table S3. Valid meteorological simulations provide a solid foundation for accurately describing the influence of meteorological conditions on long-term PM<sub>2.5</sub> pollution changes.

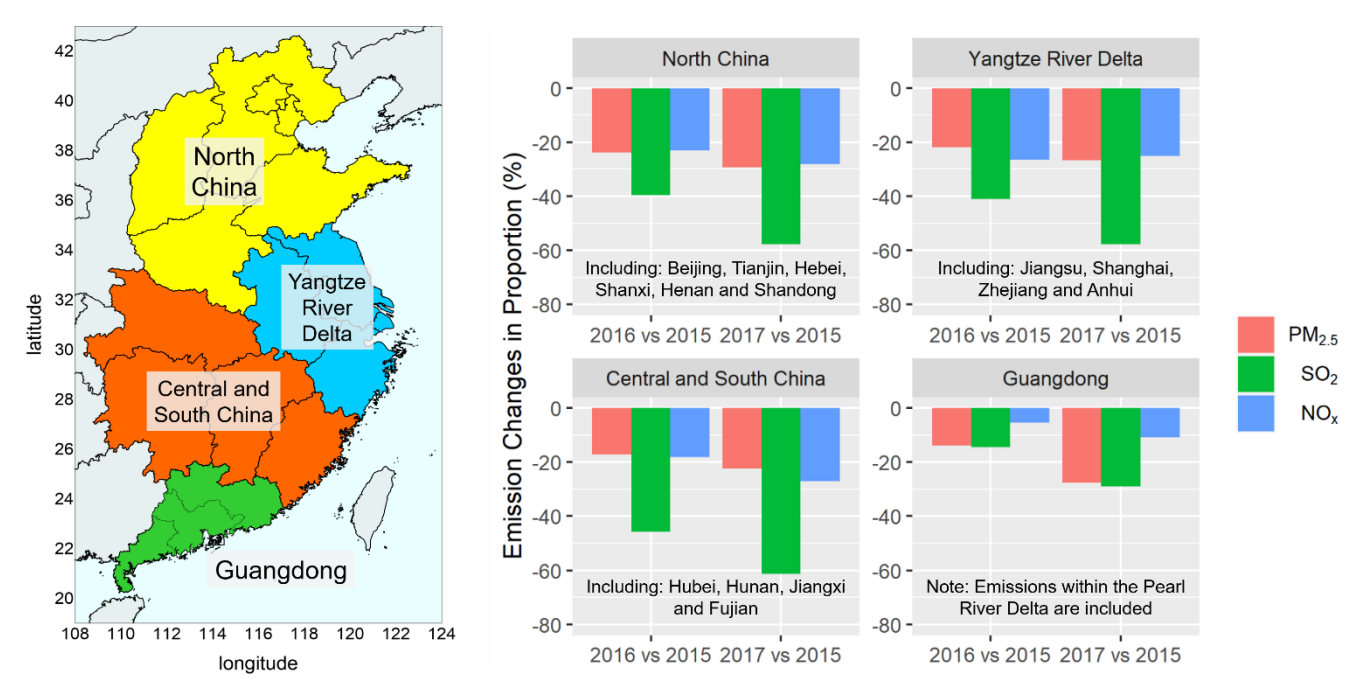


**Figure S1.** Changes in annual  $PM_{2.5}$ ,  $SO_2$  and  $NO_x$  emissions across different regions of East China (distributions shown in the left panel) in 2016 and 2017 relative to the 2015 levels.

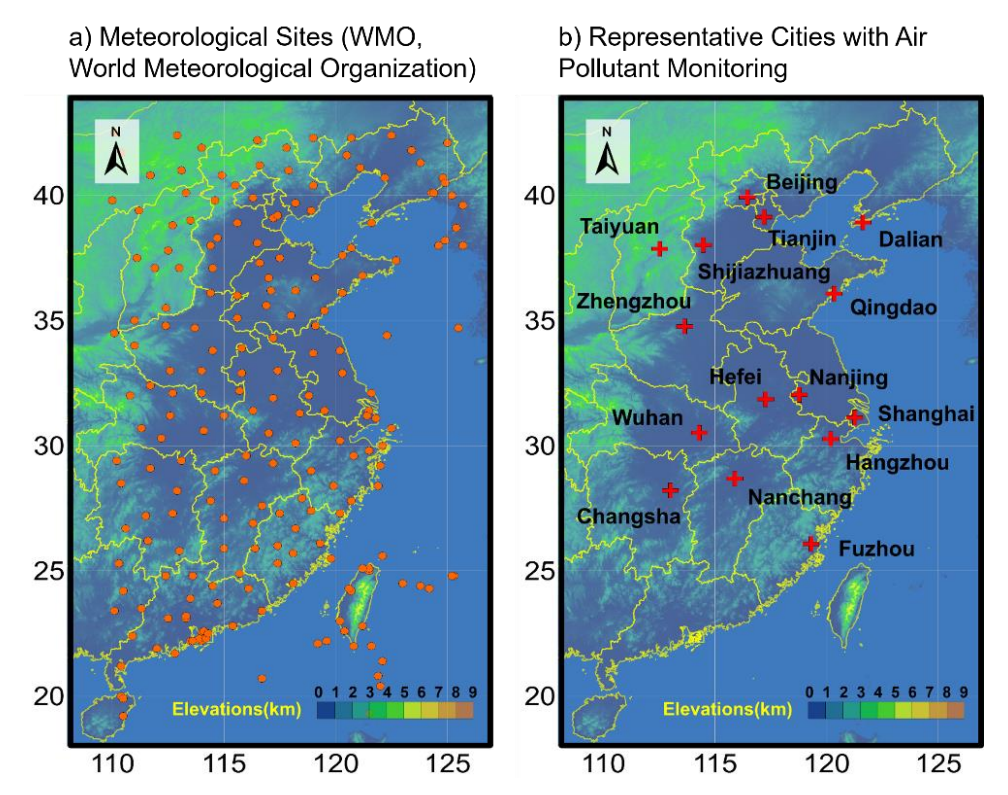


**Figure S2.** Distribution of sites or cities where the observational datasets were used in the evaluation of model performance: (a) Meteorological sites (n = 226); (b) representative cities with air quality monitoring (n = 15).

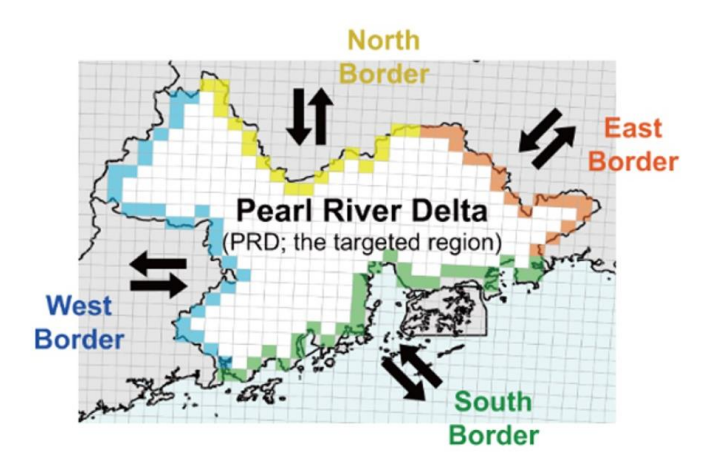
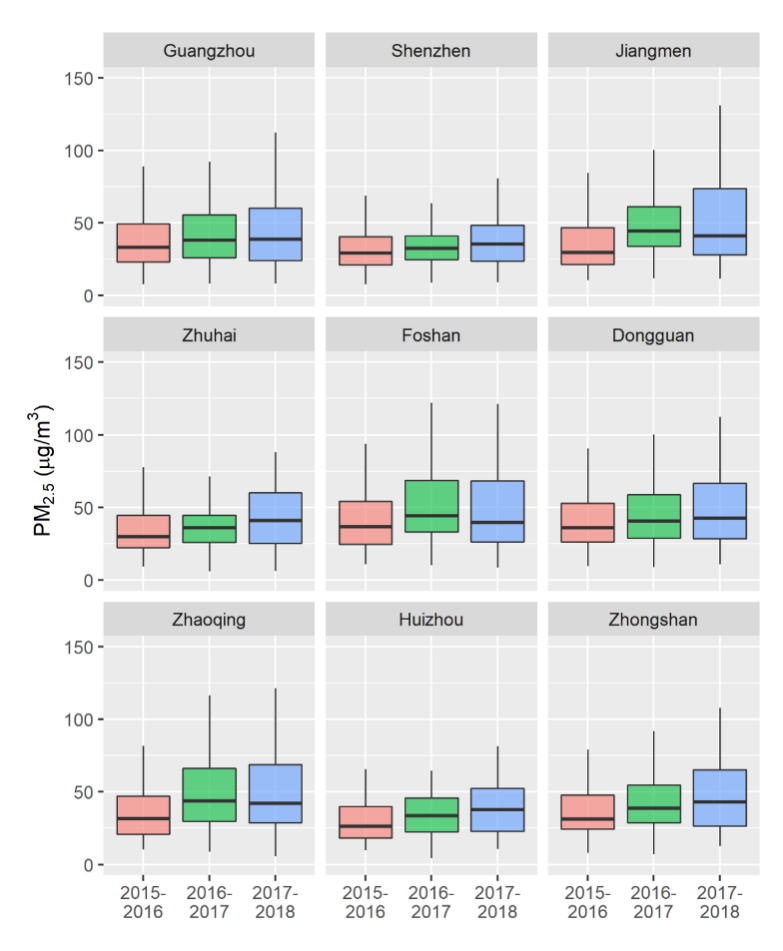
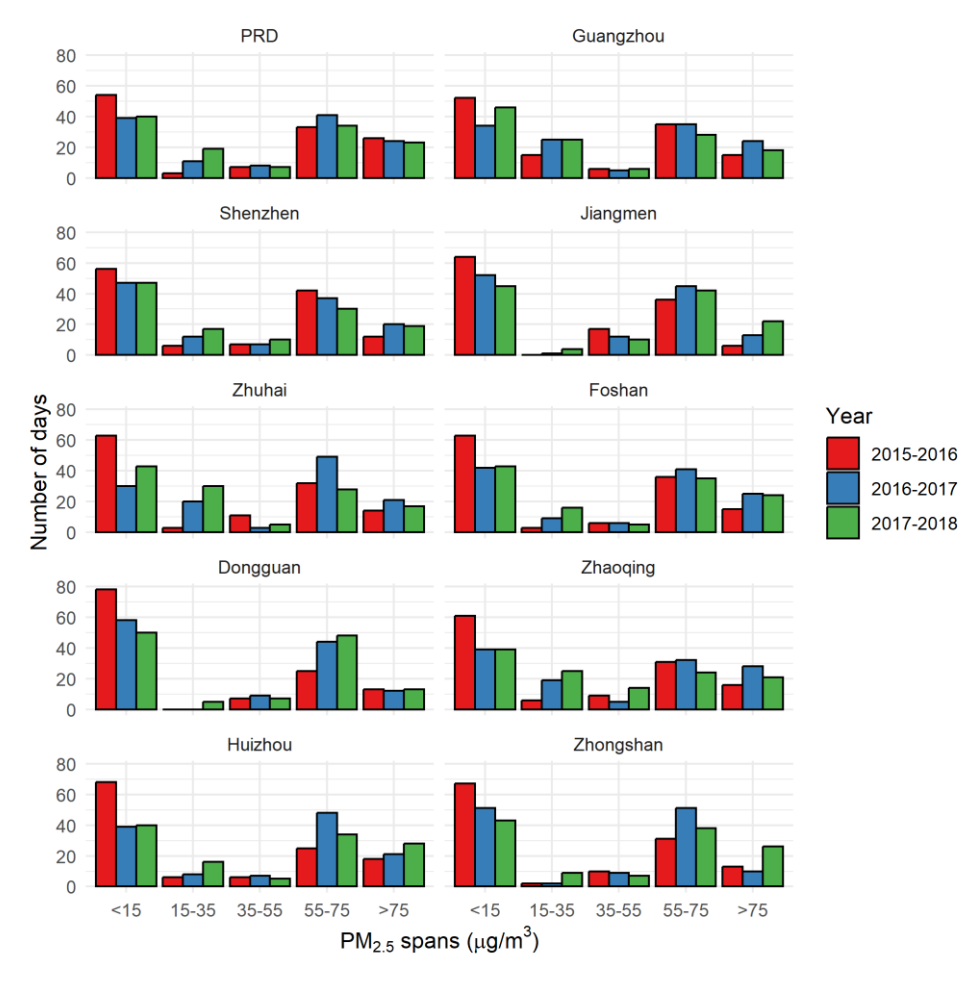


Figure S3. North, south, west, east borders of the PRD in the budget analysis (originated from Qu et al. (2023)).



**Figure S4.** Comparison of PM<sub>2.5</sub> concentrations in the nine municipalities of the PRD during the cold seasons of 2015-2017.



**Figure S5.** Number of days with various  $PM_{2.5}$  concentration spans in the PRD and its nine municipalities during the cold seasons of 2015-2017.

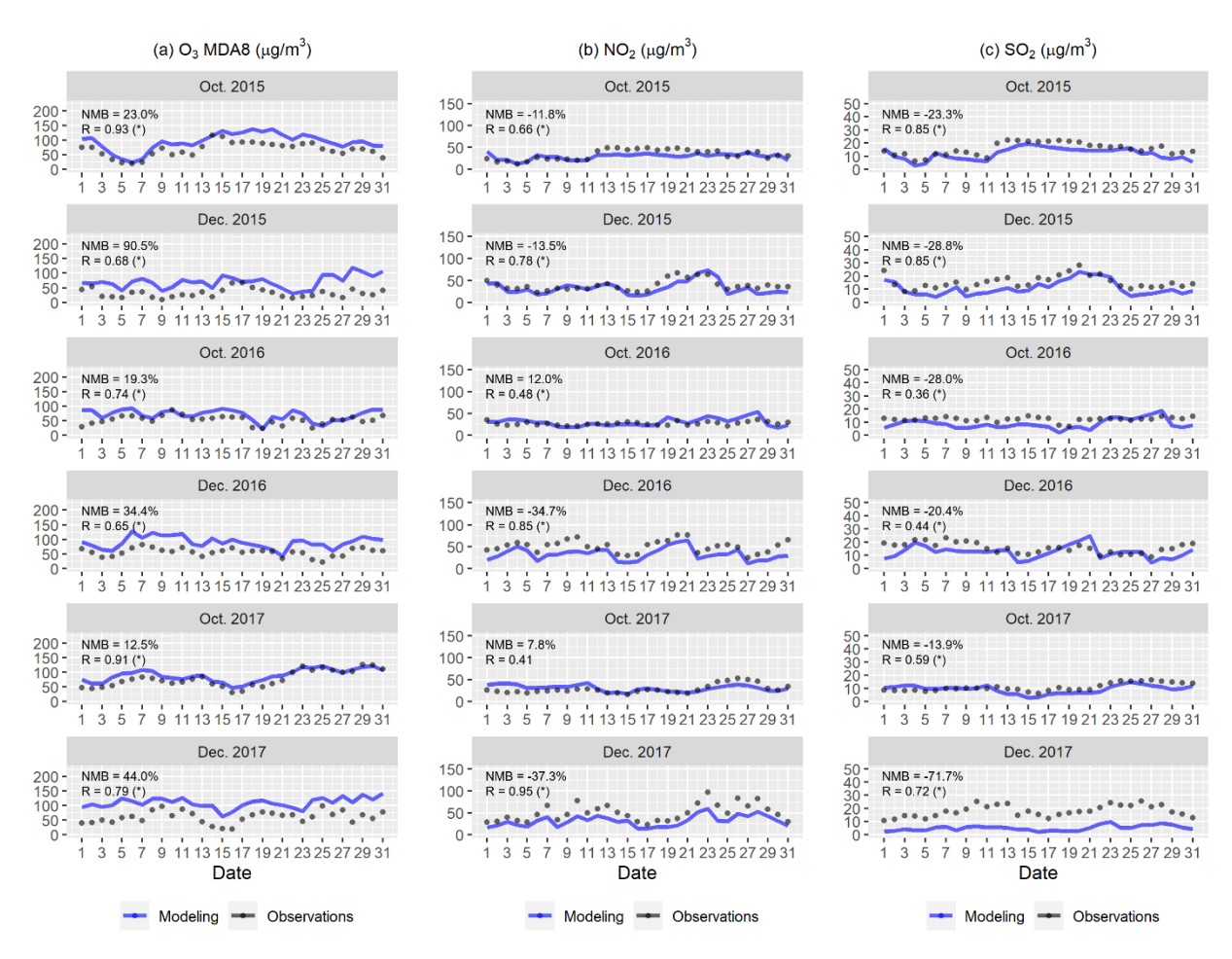


**Figure S6.** Comparisons between maximum daily 8-hour average concentrations (MDA8) of  $O_3$  (a), daily concentrations of  $NO_2$  (b) and  $SO_2$  (c) from model results and observations in the PRD. NMB, normalized mean bias; R, correlation coefficient. "(\*)" indicates that the p value is less than 0.05 for the comparisons.

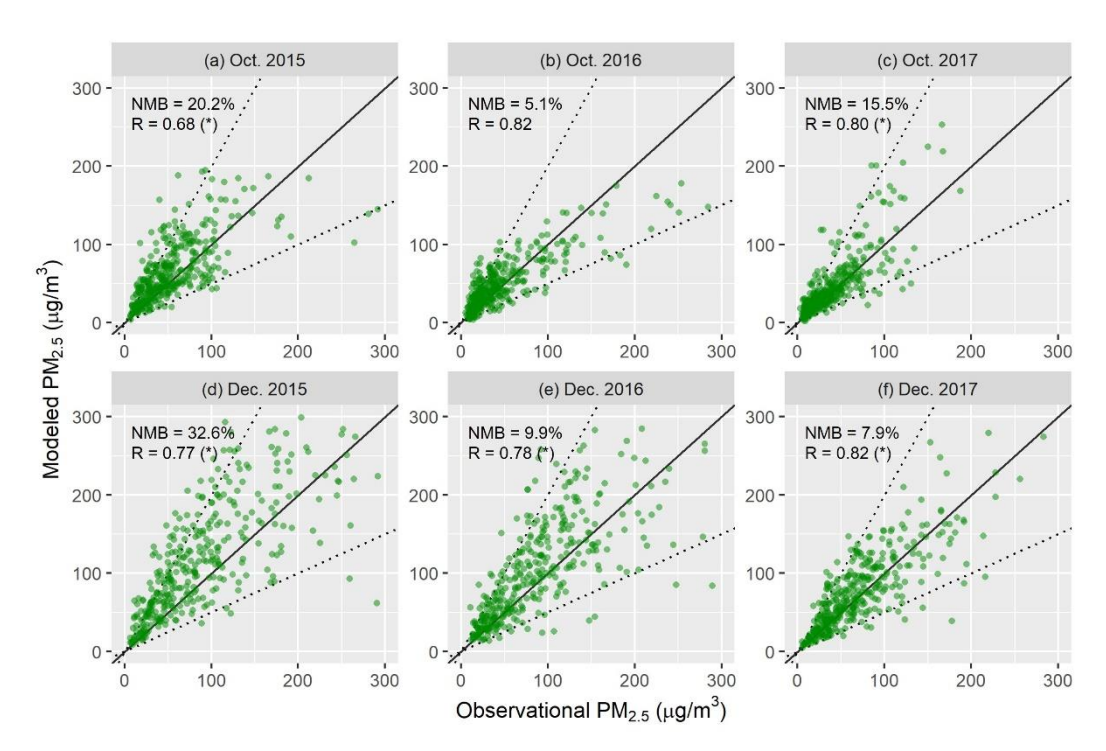


**Figure S7.** Comparisons between daily mean  $PM_{2.5}$  concentrations from model results and observations in the 15 representative cities to the north of the PRD (locations shown in Fig. S1b). NMB, normalized mean bias; R, correlation coefficient. "(\*)" indicates that the p value is less than 0.05 for the comparisons.



**Figure S8.** Comparisons of regional source contributions to population-weighted mean PM<sub>2.5</sub> sulfate (pSO<sub>4</sub>) concentrations on the PM<sub>2.5</sub> polluted days in the PRD. The scenario corresponding to each result is noted in red.



**Figure S9.** Same as Fig. S8 but for PM<sub>2.5</sub> nitrate (pNO<sub>3</sub>).



**Figure S10.** Same as Fig. S8 but for PM<sub>2.5</sub> ammonium (pNH<sub>4</sub>).

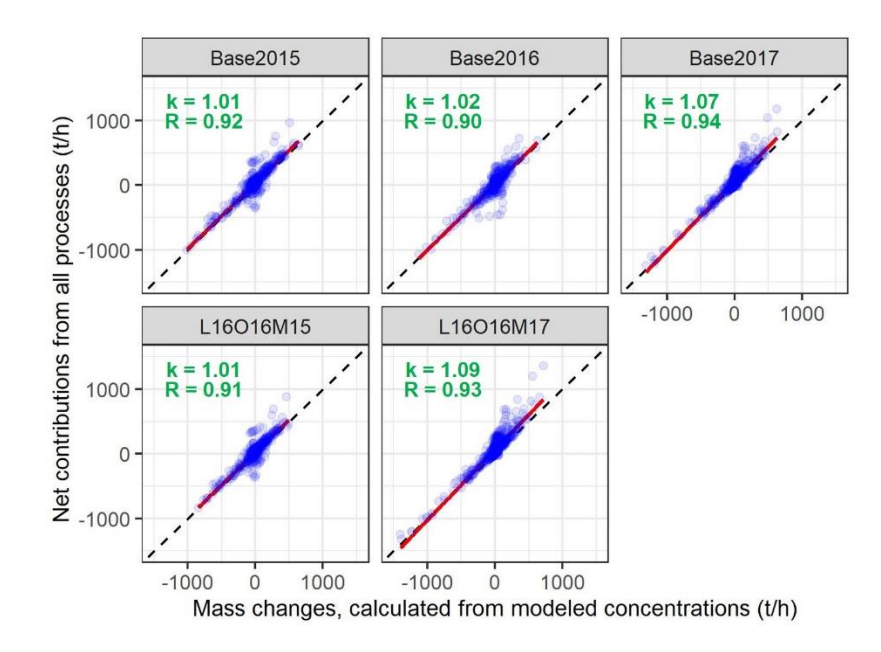


**Figure S11.** The examinations of budget conservation in the five simulation scenarios (*Base2015*, *Base2016*, *Base2017*, *L16016M15* and *L16016M17*) for the hourly PM<sub>2.5</sub> mass budgets in the PRD. The solid red lines are the fitted lines, and the dashed black lines are the 1:1 reference lines. k, slopes; R, correlation coefficient.

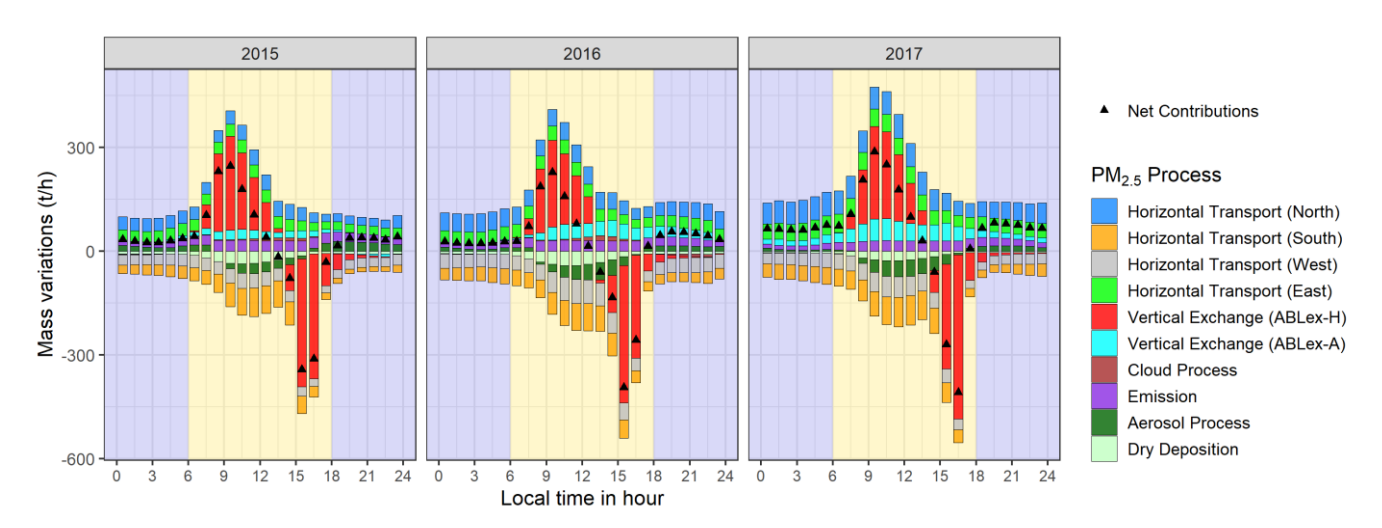


**Figure S12.** Mean diurnal variations of  $PM_{2.5}$  mass budget on the polluted days of 2015-2017 cold seasons (emissions fixed at the 2016 levels, or based on the scenarios L16016M15, Base2016 and L16016M17) within the ABL of the PRD. Backgrounds in yellow and dark blue indicate daytime and nighttime periods, respectively.

**Table S1.**  $PM_{2.5}$  polluted days in the six representative months and corresponding daily mean  $PM_{2.5}$  concentrations ("conc"; unit:  $\mu g/m^3$ ) in the PRD

Oct. 2015		Dec. 2015		Oct. 2016		Dec. 2016		Oct. 2017		Dec. 2017	
date	conc										
1	54.1	1	50.8	15	38.9	1	69.0	23	56.4	5	39.8
13	54.6	13	49.7	16	39.3	2	65.4	24	67.6	6	53.2
14	74.7	16	47.3	17	41.8	3	63.5	25	74.2	7	72.6
15	77.0	19	50.8	29	39.9	4	68.7	26	71.2	8	53.1
16	67.2	20	64.2			5	77.9	27	63.3	9	73.5
17	58.8	21	64.2			6	50.1	28	58.5	10	93.9
18	62.2	22	80.5			7	71.1	29	47.8	11	55.6
19	65.1	23	76.5			8	66.5	30	48.0	12	60.5
20	58.6	29	41.8			9	68.5	31	53.7	13	68.8
21	51.3	30	38.1			10	75.9			14	60.7
22	47.0	31	43.7			11	64.2			15	36.8
23	50.0					13	53.4			18	52.8
24	56.4					17	45.3			19	36.9
28	61.7					18	55.4			21	37.0
30	47.3					19	51.8			22	61.5
						20	59.7			23	89.5
						21	69.1			24	69.6
						24	49.2			25	65.3
						25	52.5			26	81.0
						26	55.6			27	78.5
						28	37.9			28	86.3
						29	39.8			29	78.5
						30	45.5			30	54.2
						31	63.5			31	42.6

**Table S2.** Statistical metrics used in model evaluation.  $S_m$ ,  $S_o$  indicate the values of meteorological variables or pollutant concentrations from modeling and observations, respectively, and  $\sigma_{S_m}$  and  $\sigma_{S_o}$  separately indicate their standard deviation.

Statistical metrics	Short name	Calculations
Mean Bias	MB	$\overline{S_m} - \overline{S_o}$
Gross Error	GE	$\overline{ S_m - S_o }$
Normalized Mean Bias	NMB	$\frac{\overline{S_m - S_o}}{\overline{S_o}} \times 100\%$
Root Mean Square Error	RMSE	$\sqrt{\overline{(S_m - S_o)^2}}$
Correlation Coefficient	R	$\frac{\overline{(S_m - \overline{S_m})(S_o - \overline{S_o})}}{\sigma_{S_m}\sigma_{S_o}}$
Index of Agreement	IOA	$1 - \frac{\overline{(S_m - S_o)^2}}{\overline{( S_m - \overline{S_o}  +  S_o - \overline{S_o} )^2}}$

**Table S3.** Statistical metrics in the evaluation of model performance in simulating meteorological variables. Recommend values for the metrics are from Emery et al. (2001). Results fail to meet the recommend values are marked in bold.

Variables	Metrics	Oct. 2015	Dec. 2015	Oct. 2016	Dec. 2016	Oct. 2017	Dec. 2017	Recommend values
Temperature	MB (K)	-0.26	-0.24	-0.21	-0.23	-0.28	-0.23	≤±0.5
	GE (K)	1.79	1.80	1.67	1.80	1.79	1.90	≤ 2
	IOA	0.97	0.98	0.97	0.98	0.97	0.98	$\geq 0.8$
Absolute humidity	MB (g/kg)	-0.62	-0.11	-0.67	-0.06	-0.70	-0.12	$\leq \pm 1$
,	GE (g/kg)	1.17	0.64	1.13	0.68	1.16	0.65	≤ 2
	IOA	0.97	0.98	0.98	0.98	0.97	0.98	≥ 0.6
Wind speed	MB (m/s)	0.23	0.03	-0.09	0.23	-0.06	0.05	$\leq$ $\pm 0.5$
	RMSE (m/s)	1.80	1.51	1.68	1.30	1.70	1.46	≤ 2
	IOA	0.80	0.85	0.81	0.80	0.84	0.81	≥ 0.6
Wind direction	MB (°)	4.10	2.97	1.19	3.44	0.92	2.10	$\leq$ $\pm 10$
	GE (°)	33.53	30.19	30.51	34.28	29.49	33.57	≤ 30

**Table S4.** Comparisons of simulated AdjGR and  $\epsilon(pNO_3)$  in the PRD in five scenarios.

Scenarios	AdjGR	ε(pNO <sub>3</sub> )
Base2015	2.29	70.6%
Base2016	2.94	67.7%
Base2017	2.91	61.7%
L16O16M15	2.63	69.8%
L16O16M17	2.79	63.1%

## References

- Borge, R., Alexandrov, V., José del Vas, J., Lumbreras, J., and Rodríguez, E.: A comprehensive sensitivity analysis of the WRF model for air quality applications over the Iberian Peninsula, Atmos. Environ., 42, 8560–8574, https://doi.org/10.1016/j.atmosenv.2008.08.032, 2008.
- Emery, C., Tai, E., and Yarwood, G.: Enhanced Meteorological Modeling and Performance Evaluation for Two Texas Ozone Episodes, Prepared for the Texas Natural Resource Conservation Commission, Environ International Corporation, Novato, CA, 2001.
- Hu, J., Chen, J., Ying, Q., and Zhang, H.: One-year simulation of ozone and particulate matter in China using WRF/CMAQ modeling system, Atmos. Chem. Phys., 16, 10333–10350, https://doi.org/10.5194/acp-16-10333-2016, 2016.
- Qu, K., Wang, X., Cai, X., Yan, Y., Jin, X., Vrekoussis, M., Kanakidou, M., Brasseur, G. P., Shen, J., Xiao, T., Zeng, L., and Zhang, Y.: Rethinking the role of transport and photochemistry in regional ozone pollution: insights from ozone concentration and mass budgets, Atmos. Chem. Phys., 23, 7653–7671, https://doi.org/10.5194/acp-23-7653-2023, 2023.
- Wang, X., Zhang, Y., Hu, Y., Zhou, W., Lu, K., Zhong, L., Zeng, L., Shao, M., Hu, M., and Russell, A. G.: Process analysis and sensitivity study of regional ozone formation over the Pearl River Delta, China, during the PRIDE-PRD2004 campaign using the Community Multiscale Air Quality modeling system, Atmos. Chem. Phys., 10, 4423–4437, https://doi.org/10.5194/acp-10-4423-2010, 2010.
- Zhang, H., Li, J., Ying, Q., Yu, J. Z., Wu, D., Cheng, Y., He, K., and Jiang, J.: Source apportionment of PM<sub>2.5</sub> nitrate and sulfate in China using a source-oriented chemical transport model, Atmos. Environ., 62, 228–242, https://doi.org/10.1016/j.atmosenv.2012.08.014, 2012.